Received: 21 December 2021 | Accepted: 2 June 2022

DOI: 10.1111/ene.15452

european journal of neurology
the official journal of the european academy of neurology

ORIGINAL ARTICLE

GNA11-mutated Sturge–Weber syndrome has distinct neurological and dermatological features

Anne Dompmartin[1] | Carine J. M. van der Vleuten[2] | Valérie Dekeuleneer[3] | Thierry Duprez[4] | Nicole Revencu[5] | Julie Désir[6] | D. Maroeska W. M. te Loo[7] | Uta Flucke[8] | Astrid Eijkelenboom[8] | Leo Schultze Kool[9] | Miikka Vikkula[10] | Laurence Boon[3]

[1]Service Dermatologie CHU, Université Caen Normandie, Caen, France

[2]Dermatology & Center for Vascular Anomalies, University Medical Center Nijmegen, Nijmegen, The Netherlands

[3]Division of Plastic Surgery, Cliniques Universitaires Saint-Luc, Center for Vascular Anomalies, Brussels, Belgium

[4]Radiology, Cliniques universitaires Saint-Luc, Brussels, Belgium

[5]Human Genetics, Cliniques universitaires Saint-Luc, Brussels, Belgium

[6]Erasmus Hospital, Human Genetics, Brussels, Belgium

[7]Radboudumc, Pediatric Haematology & Center Vascular Anomalies, Nijmegen, The Netherlands

[8]Radboudumc, Pathology & Center for Vascular Anomalies, Nijmegen, The Netherlands

[9]Radboudumc, Radiology & Center for Vascular Anomalies, Nijmegen, The Netherlands

[10]Human Molecular Genetics, de Duve Institute, UCLouvain, Brussels, Belgium

Correspondence
Laurence Boon, Division of Plastic Surgery, Center for Vascular Anomalies, University Clinics Saint-Luc, University of Louvain, Avenue Hippocrate 10, B-1200 Brussels, Belgium.
Email: laurence.boon@uclouvain.be

Funding information
Fonds De La Recherche Scientifique - FNRS, Grant/Award Number: T.0026.14 and T.0146.16; Koning Boudewijnstichting, Grant/Award Number: GENERET PRICE 2018

Abstract

Background and purpose: Sturge–Weber syndrome (SWS) is a neurocutaneous disorder characterized by clinical manifestations involving the brain, eye and skin. SWS is commonly caused by somatic mutations in *G protein subunit Alpha Q* (*GNAQ*). Five cases of *subunit Alpha 11* (*GNA11*) mutations have been reported. We studied phenotypic features of GNA11-SWS and compared them with those of classic SWS.

Methods: Within two European multidisciplinary centers we looked for patients with clinical characteristics of SWS and a *GNA11* mutation. Clinical and radiological data were collected retrospectively and prospectively.

Results: We identified three patients with SWS associated with a somatic *GNA11* mutation. All had disseminated capillary malformation (CM) and hyper- or hypotrophy of an extremity. At birth, the CMs of the face, trunk and limbs were pink and patchy, and slowly darkened with age, evolving to a purple color. Two of the patients had glaucoma. All had neurological symptoms and moderate brain atrophy with a lower degree of severity than that classically associated with SWS. Susceptibility-weighted imaging (SWI) and contrast-enhanced fluid-attenuated inversion recovery (FLAIR) magnetic resonance imaging demonstrated the best sensitivity to reveal the pial angiomas.

Conclusions: We have differentiated two distinct clinical/radiological phenotypes of SWS; GNAQ- and GNA11-SWS. The classic GNAQ-SWS is characterized by a homogeneous dark-red CM, commonly associated with underlying soft tissue hypertrophy. The CM in GNA11-SWS is more reticulate and darkens with time, and the neurological picture is milder. SWI and post-contrast FLAIR sequences appear to be necessary to demonstrate leptomeningeal angiomatosis. Anti-epileptic medication or future targeted therapies may be useful, as in classic SWS.

KEYWORDS
neurocutaneous syndrome, port-wine stain, SWS = Sturge–Weber syndrome, hypertrophy, mutation

Anne Dompmartin and Carine J. M. van der Vleuten equally contributed to this work.

INTRODUCTION

Sturge–Weber syndrome (SWS) is a neurocutaneous disorder the features of which are a triad of clinical manifestations involving the brain, eye, and skin [1]. It is characterized by a facial capillary malformation (CM; "port-wine" stain) of the eyelid and forehead [2]. Most patients develop glaucoma in the eye adjacent to the CM [3]. SWS is associated with a capillary or venular malformation of the leptomeninges (leptomeningeal angiomatosis), which is the major criterion for the diagnosis [4]. Patients with leptomeningeal angiomatosis without skin and/or eye involvement are diagnosed as having intracranial SWS [5]. The CM in SWS can be limited to the face, contiguously or not with a CM on the neck, trunk and/or extremities. SWS is associated with hypertrophy of an extremity in 14% of patients [6].

Since the princeps paper in 2009, various vascular anomalies have been identified to be associated with somatic or mosaic mutations [7–9]. SWS is one of these, found to be associated with a somatic activating mutation in *GNAQ* ("GNAQ-SWS") in most patients, similar to common facial CM [10]. A somatic *GNA11* mutation was reported in four patients with SWS and in two patients with CM with glaucoma without neurological symptoms or normal magnetic resonance imaging (MRI) [11–14]. Detailed description of the clinical and/or radiological features of these patients was not provided. [11–14]

Within two multidisciplinary centers of the working group on vascular anomalies (VASCA) of the European Reference Network on Multisystemic Vascular Diseases (VASCERN) (https://vascern.eu/), we identified three patients with clinical characteristics of SWS associated with a somatic *GNA11* mutation. They all had disseminated CM and hyper- or hypotrophy of an extremity. For these three cases, we describe *GNA11*-mosaicism-based SWS ("GNA11-SWS") in which there is a distinctive clinical and radiological presentation and evolution over time.

MATERIALS AND METHODS

Standard protocol approvals, registrations, and patient consents

Informed consent was obtained from all patients after clearance of the study by the Biomedical Ethics Committees of the University of Louvain, Brussels, Belgium, and the Radboud University, Nijmegen, the Netherlands.

Clinical data

Clinical records and photographs were reviewed. Patients were re-contacted for clinical re-evaluation and MRI imaging.

Genetic analyses

For all cases, lesional biopsies were collected in RNALater solution. For Case 1, leftover tissue from a programmed therapeutic surgery was also collected, snap-frozen in liquid nitrogen. DNA extraction was performed as previously described using a Wizard genomic DNA purification kit (Promega, Madison, WI, USA) [15]. DNA was quantified using NanoDrop 8000 (Thermo Fisher Scientific, Waltham, MA, USA) and Qubit 2.0 (Thermo Fisher Scientific).

Sequencing

DNA was screened using Ion Torrent technology, with a custom Ampliseq panel (www.ampliseq.com) designed to cover the coding exons of *GNAQ* and *GNA11*. Reads were aligned to the human reference sequence hg19, using the Torrent Suite Server. Bam files were imported into Highlander software package (https://sites.uclouvain.be/highlander/) for analysis. We selected variants with at least five mutant reads, representing at minimum 1% of all alleles.

Imaging

Brain MRI examination was available in all three patients. Only one of these had additional unenhanced cerebral computed tomography (CT) images. MRI work-up in all patients included conventional T2-weighted images and three-dimensional (3D) susceptibility-weighted imaging (SWI) acquisition using the blood level oxygen-dependent (BOLD) effect, resulting in strong darkening within desaturated slow-flow veins. Two patients had also contrast-enhanced T1-weighted views and one had additional contrast-enhanced 3D fluid-attenuated inversion recovery (FLAIR) views.

RESULTS

Case 1

Case 1 is a 44-year-old White man, born with a whole-body patchy CM on the face, trunk, and upper and lower limbs (Figure 1, Table 1). The CM darkened over time, being pale pink at birth, becoming pink in childhood, and having evolved into a dark red purple patch, as of today (Figure 1a–d). There is no vascular nodule on the CM, but the CM is strongly reticulated on both hands (Figure 1d). The CM is associated with girth hypertrophy (+3 cm) of the left thigh and buttock, varicose veins and ulcers related to venous insufficiency. At the age of 7 years, severe and recurrent seizures refractory to optimized anti-epileptic medical treatment appeared and the patient developed right-sided hemiplegia and progressive dysphasia. The patient has had bilateral glaucoma

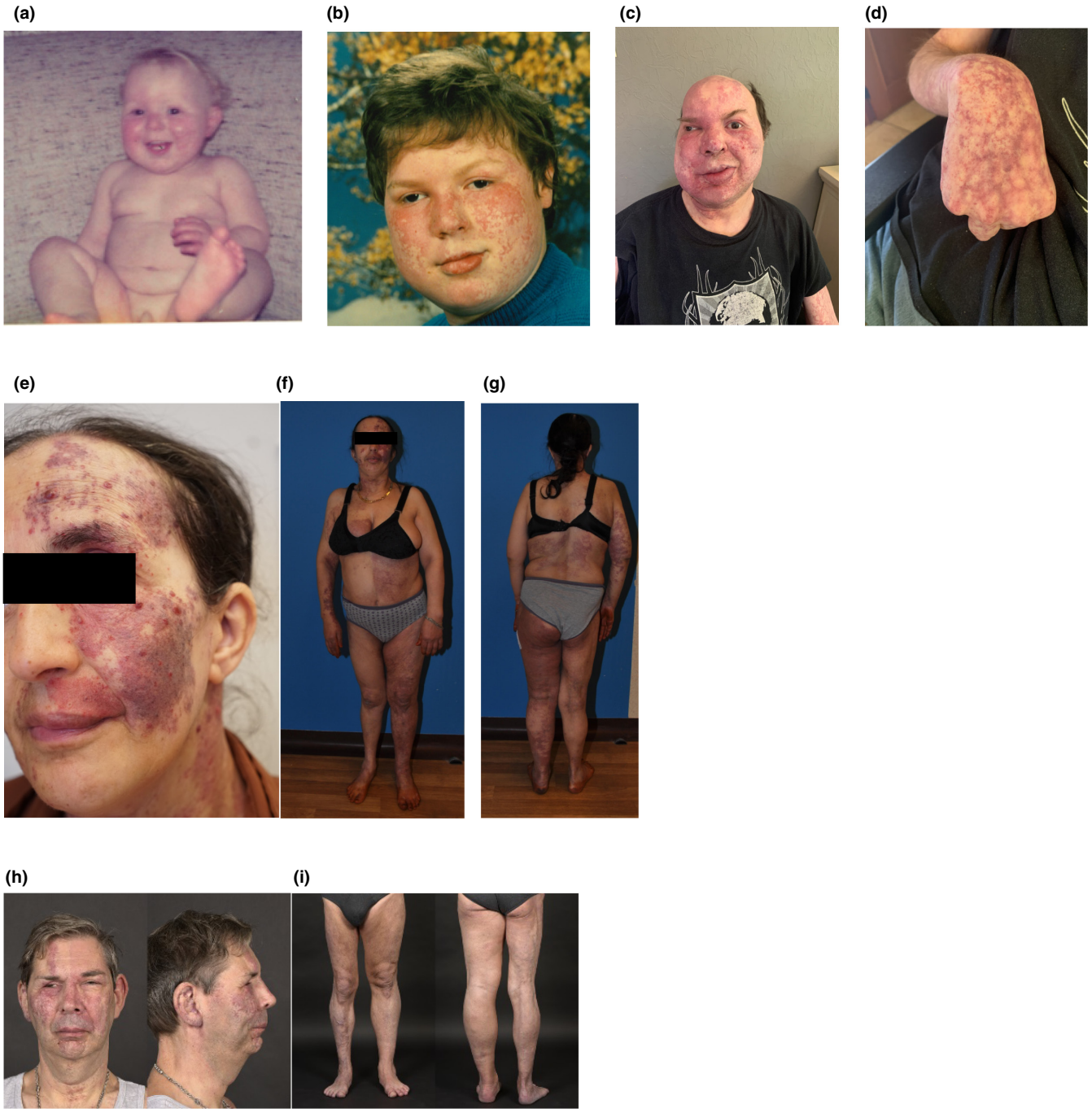

FIGURE 1 Clinical photographs of patients showing extensiveness of capillary malformation (CMs). Evolution of color of cutaneous CMs from pale pink (a–d) to purple with age. Patient 1: (a) age 6 months; (b) age 12 years; (c) age 40 years; (d) area of reticulated CM. Patient 2; (e) dark CM with rare nodules on the face; (f) and (g) CM spread on half of the body. Patient 3; (h) and (i), dark CM. (i) hypotrophy of right lower extremity

since birth, leading to blindness in the right eye. Complementary investigations revealed primary hypothyroidism, several episodes of gastrointestinal bleeding of unknown origin, high blood pressure, and asthma. The brain MRI performed at the age of 16 years (in 1991) demonstrated only moderate atrophy of the left cerebral hemisphere without focal brain tissue change (Figure 2a). On a later MRI work-up, conventional post-contrast T1-weighted views failed to reveal a pial angioma (Figure 2b), the presence of which was indirectly revealed by enlargement of deoxygenated afferent cortical veins seen clearly on SWI using the BOLD effect (Figure 2c). Molecular analyses of two affected skin samples revealed a *GNA11* mutation (p.Arg183Cys; Table 1).

Case 2

Case 2 is a 51-year-old Maghrebin woman, born with a pale pink extensive patchy CM of the face (V1,2,3), left part of the trunk, and left

TABLE 1 Clinical findings in patients

			Case 1 GNA11-SWS	Case 2 GNA11-SWS	Case 3 GNA11-SWS	"Classic" GNAQ-SWS	DCMO
CM	Color	At birth	**Pale pink**	**Pale pink**	**Extensive; exact color difficult to retrive**	**Bright red**	**Pale pink**
		In adulthood	**Purple**	**Purple**	**Purple**	**Dark red**	**More pale pink**
	Localization	Nodules	**No**	**3**	**No**	**Multiple nodules during lifetime**	**No**
		Head and neck	Whole face	Left hemiface	Both sides of the face (right side more affected)	Forehead ++, median forehead, hemifacial	No specific location
		Thoracodorsal	Bilateral	Left	Trunk, bilateral	Possible	Extensive
		Upper limb	Bilateral	Right	Arms, bilateral	Possible	extensive
		Lower limb	Bilateral	Left	Right leg	14%	Extensive
	Aspect		**Patchy**	**Patchy**	**Patchy**	**Homogeneous plaques**	**Reticulated**
Associated signs and symtoms of lower extremities		Hypotrophy	**No**	**No**	**Right leg**	**No**	**No**
		Hypertrophy	**Left thigh and buttock**	**Left leg**	**No**	**Face**	**Underlying CM, variable**
		Varicose veins	Yes	Yes	Yes	Possible	Possible
		White, atrophy	No	No	Yes	Possible	No
		Ulcer	Yes	No	Yes with bleeding	Possible	No
		Leg length discrepancy using X-ray	Left leg 3.8 cm > right leg	Left leg 2.0 cm > right leg	Left leg 3.8 cm > right leg (persisting after orthopedic correction at age 18 years)	Possible	Possible
Associated neurological signs and symptoms		Epilepsy	**Severe in middle childhood, refractory to anti-epileptic medication**	**Mild in adulthood, good response to anti-epileptic medication**	**No**	**Severe in infancy**	**No**
		Neurological symptoms	Pyramidal syndrome, severe epilepsy, progressive epileptic dysphasia, spastic right hemiparesis	Dizziness, nausea, vomiting due to epilepsy crisis, cervicobrachial neuralgia	Migraine with aura	Seizures, stroke-like episodes, developmental delay	No
		Brain MRI	**Light hemispheric atrophy - pial angioma revealed indirectly by SWI-BOLD**	**Moderate hemispheric atrophy - pial angioma revealed indirectly by SWI-BOLD and well depicted on post-contrast FLAIR**	**Light hemispheric atrophy - pial angioma revealed by SWI-BOLD**	**Leptomeningeal angiomatosis <1 year**	**na**

TABLE 1 (Continued)

		Case 1 GNA11-SWS	Case 2 GNA11-SWS	Case 3 GNA11-SWS	"Classic" GNAQ-SWS	DCMO
		Prominent cortical vein dilatation / slow flow	**Prominent cortical vein dilatation / slow flow**	**Prominent cortical vein dilatation / slow flow**	**Usual prominence of radial transmedullary veins**	**na**
	Brain CT scanner	Not available	Parenchymal and pial calcifications	Not available	Calcifications	na
Glaucoma		Congenital, bilateral	No	Right eye; blind	Yes	Possible
Somatic mutation: gene	Biopsy on the CM	***GNA11***	***GNA11***	***GNA11***	***GNAQ***	***PIK3CA***
Somatic mutation	Mutant allele fraction	c.547C > T p.Arg183Cys (NM_002067.4) CM thorax: 15% CM buttock: 9%	c.547C > T p.Arg183Cys (NM_002067.4) CM thorax: 4,1%	c.547C > T p.Arg183Cys (NM_002067.4) CM face: 18% CM leg: 7%	Variable, often <10%	Variable, often <10%
Thyroide	Thyroide Exploration	Central hypothyroidism	Autoimmune thyroiditis	Autoimmune thyroiditis	<3% central hypothyroidism	No
Imaging	Leg MRI	Not done	Dilated veins, subcutaneous hypertrophy, no vascular malformation	Not done	na	na

Abbreviations: BOLD, blood level oxygen-dependent; CM, capillary malformation; CT, computed tomography; DCMO, diffuse capillary malformation with overgrowth; FLAIR, fluid-attenuated inversion recovery; MRI, magnetic resonance imaging; na, not applicable; SWI, susceptibility-weighted imaging; SWS, Sturge–Weber Syndrome.

Bold: Features that help distinguish GNA11-SWS from GNAQ-SWS and DCMO.

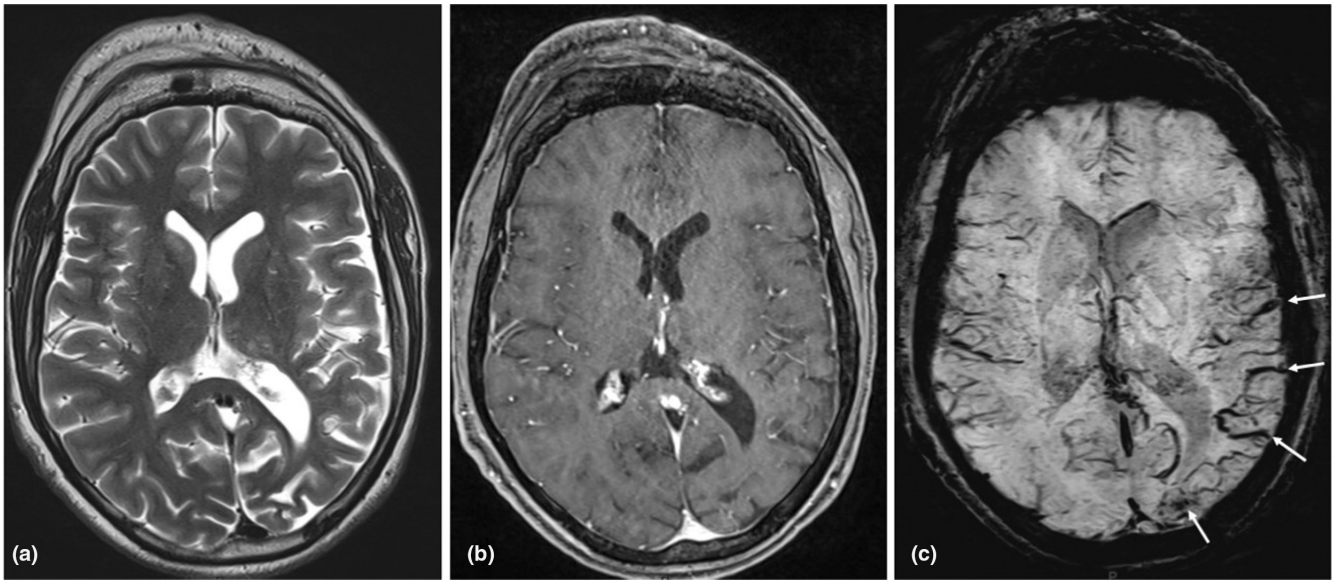

FIGURE 2 Magnetic resonance imaging (MRI) work-up of Patient #1. Axial-transverse views in similar slice location. (a) T2-weighted view revealing left frontal–parietal atrophy with sulcal enlargement without intrinsic parenchymal tissue changes. (b) Contrast-enhanced T1-weighted view failing to reveal left pial hemangioma. (c) Susceptibility-weighted imaging view revealing left-sided frontal–parietal pial abnormality through darkening blood level oxygen-dependent effect within enlarged slow-flowing desaturated veins (arrows)

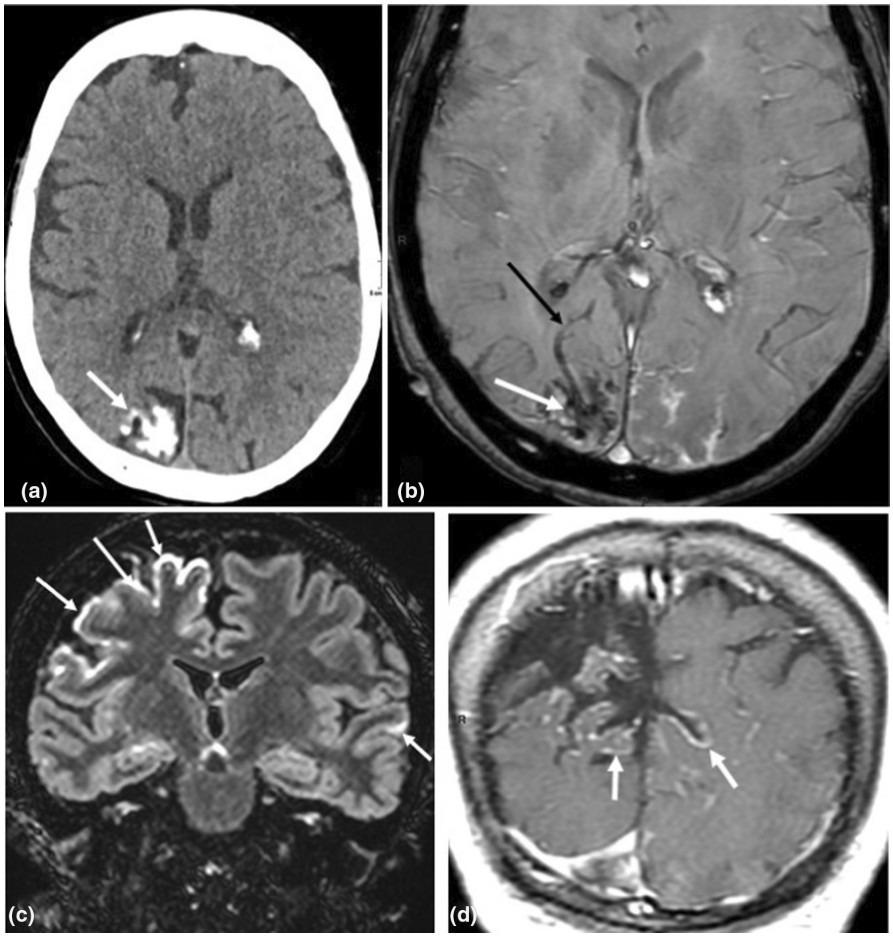

FIGURE 3 Computed tomography (CT) and magnetic resonance imaging (MRI) work-up of Patient #2: (a) non-contrast CT scan view, (b–d) contrast-enhanced MRI views. (a) Axial-transverse slice revealing hyperdense calcium deposits in the right parietal lobe (arrow). (b) Axial-transverse susceptibility-weighted imaging with blood level oxygen-dependent (BOLD) effect slice (magnified view), in similar slice location to (a), showing darkening susceptibility effects in the right parietal lobe due to calcium deposits (white arrow) together with enlarged afferent vein (black arrow) of which darkening is attributable to the BOLD effect. (c) Coronal fluid-attenuated inversion recovery view showing intense enhancement of the pial angioma involving mainly the right cerebral hemisphere (arrows). (d) Coronal T1-weighted view in more posterior location than (c) showing only faint abnormal pial enhancement in both parietal lobes (arrows). Observe right focal atrophy of brain tissue

lower and right upper limbs. The CM darkened with age and is now red purple in color and strongly reticulated on the trunk (Table 1, Figure 1e–g). There are three vascular nodules, together with varicose veins, and length (2.1 cm L > R at scaniometry) and girth hypertrophy of the left lower limb (Figure 1f,g). There is no glaucoma, but she experiences neurological symptoms including dizziness,

nausea and vomiting, which started at 49 years of age. She also has autoimmune thyroiditis, cervicobrachial neuralgia, arthralgia and splenomegaly. Brain CT scan revealed dense calcium deposits within the brain parenchyma of the right occipital lobe, together with obvious hypoplasia/atrophy of the homolateral cerebral hemisphere (Figure 3a). T1/T2-weighted MRI confirmed brain atrophy, whereas post-contrast T1-weighted and, more sensitively, contrast-enhanced FLAIR images highlighted extensive and multifocal pial angioma (Figure 3c,d). SWI-BOLD views were also contributive, demonstrating calcium deposits and an enlarged vein (Figure 3b). Limb MRI confirmed the presence of varicose veins and detected no deep vascular malformation (not shown). Molecular analyses of an affected skin sample of the thigh revealed a *GNA11* mutation (p.Arg183Cys; Table 1).

Case 3

Case 3 is a 58-year-old White man, born with extensive CM involving the face, both arms, the trunk, and the right leg. The CM was red in color at birth, and darkened with time, becoming red/purple in color with bier spots on both arms (Table 1, Figure 1h,i). He developed five vascular nodules (clinical spectrum of pyogenic granuloma) on the CM. He developed glaucoma of the right eye by the age of 6 years. He has no epilepsy, but has presented, since childhood, with occasional attacks of migraine with aura. He has girth and length hypotrophy of the right leg (3 cm L > R), which was orthopedically corrected at the age of 18 years. He has extensive varicose veins and a scar from a venous ulcer. He complains of restless and tired legs. He also has isolated essential hypertension, and autoimmune thyroiditis. Brain MRI without contrast agent perfusion performed at the age of 56 years showed moderate atrophy of the right cerebral hemisphere without parenchymal signal intensity change (Figure 4a). The presence of the pial angioma was revealed by afferent enlarged cortical veins containing desaturated hemoglobin, resulting in a strongly darkening BOLD effect on SWI (Figure 4b,c) In addition, the choroid plexus within the right lateral ventricle was enlarged when compared to the left (not shown). Duplex Doppler of the legs showed normal position of the deep and superficial venous system, but with the presence of intramuscular varicous veins on the right leg (m. biceps femoris lateralis). Molecular analyses of two affected skin samples revealed a *GNA11* mutation (p.Arg183Cys; Table 1).

DISCUSSION

Sturge–Weber syndrome is a rare, sporadic neurocutaneous syndrome. It classically features a facial CM, soft tissue and/or bony overgrowth, ipsilateral leptomeningeal angiomatosis and angioma involving the ipsilateral eye [16]. Recent studies have demonstrated that hemifacial, forehead, and midline forehead CM are associated with increased risk of SWS. Location on the forehead is the strongest independent predictor of SWS risk [17]. Classic SWS has a variable but usually progressive course in early childhood, characterized by seizures, stroke-like episodes, headaches, neurological and cognitive deterioration, hemiparesis, glaucoma and visual field defects. This syndrome is usually caused by a GNAQ mutation [10]. We suggest that classic SWS be termed "GNAQ-SWS".

The three patients in our report had a large facial CM, including on the forehead, without underlying tissue overgrowth and a pial angioma consistent with the clinical-radiological diagnosis of SWS, together with patchy reticulated CM of the trunk and limbs with

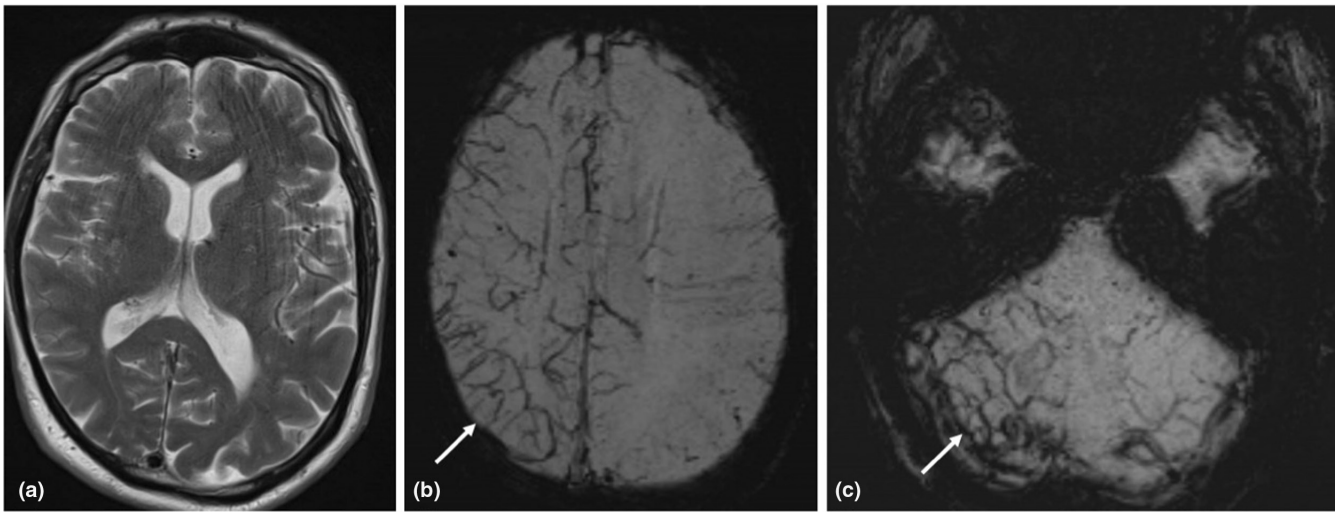

FIGURE 4 Magnetic resonance imaging (MRI) work-up of Patient #3. (a) Axial-transverse T2-weighted view showing only minor atrophy of the right cerebral hemisphere without intrinsic signal abnormality and paradoxical enlargement of left sulci. (b) Axial-transverse susceptibility-weighted imaging (SWI) with blood level oxygen-dependent (BOLD) effect view through the supra-tentorial space demonstrating right-sided strong BOLD effect-related decrease in signal intensity of slow-flow and desaturated cortical veins (arrow). This indirectly suggests the presence of the pial angioma impeding the leptomeningeal venous outflow. (c) Axial-transverse SWI-BOLD view through the infra-tentorial space demonstrating similar features in the posterior fossa to those observed in the supra-tentorial space (see b)

hyper- or hypotrophy. The CMs were pale pink at birth and typically darkened with age to become dark red/purple. Vascular nodules developed on the CMs only rarely. Two of the patients had glaucoma. There were some reticulated areas devoid of cutaneous atrophy, which allows these lesions to be differentiated from CMTC, which is characterized by a reticulated erythema associated with cutaneous atrophy. All three had autoimmune thyroiditis/primary hypothyroidism in contrast to the central hypothyroidism that can be observed in GNAQ-SWS [18]. In all three patients the capillary malformations had the same somatic hotspot *GNA11* mutation.

In addition to involvement of the face, our patients with clinical characteristics of SWS also had a CM of extremity with over- or undergrowth (SWS + CMO or + CMU). At birth and in childhood, SWS + CMO/U can mimic diffuse capillary malformation with overgrowth (DCMO), a pale disseminated reticulated or more homogeneous CM extending beyond anatomical regions. The CM of DCMO lightens with time and is associated with hypertrophy of variable areas with CM. DCMO can co-occur with glaucoma, but is not associated with SWS [19]. Its evolution also differs from SWS, as the color of the CM darkens with time in SWS + CMO or + CMU. As it is difficult to predict how the color of a CM will evolve, brain MRI can help in differential diagnosis. Based on our data, somatic genetic testing can also be used for precise diagnosis and to guide management. SWS + CMO/U is associated with a mosaic hotspot *GNA11* mutation, whereas DCMO is associated with mosaic non-hotspot *PIK3CA* mutations [20].

Brain MRI findings in our three adult patients were similar to those of GNAQ-SWS: a pial angioma, together with atrophy of the underlying cerebral parenchyma (Figures 2–4). However, the main discrepancy was a considerably lower degree of severity of the intracranial involvement in our patients when compared to GNAQ-SWS patients, in whom initial MRI work-up is frequently performed at an early pediatric age with precociously detectable lesions.

The pial angioma was strongly suspected on SWI-BOLD images (Figures 2c, 3b and 4b,c) and unequivocally demonstrated on contrast-enhanced FLAIR images (Figure 3c). SWI-BOLD strongly highlights slow-flow-related blood deoxygenation within veins due to the susceptibility effects of the deoxyhemoglobin. Use of the FLAIR technique after contrast agent perfusion synergistically enhances the contrast between the signal suppression ("blackening") of the cerebrospinal fluid and the strong increase in signal intensity of the diseased pial areas (Figure 3c). Both techniques should therefore be systematically included in the MRI work-up protocol of all SWS-suspected patients as previously advocated by others [21,22]. This requirement is re-enforced in patients with suspicion for GNA11-SWS who have milder endocranial changes than patients with GNAQ-SWS. Conventional post-contrast T1-weighted views were negative in one of our cases (Figure 2b) and only moderately positive in another (Figure 3d), which highlights a significant risk of missing the condition if SWI and contrast-enhanced FLAIR are not performed.

An additional imaging feature in all three patients was the absence of brain tissue damage within affected areas on conventional T2-weighted (Figures 2a and 4a) or FLAIR images (Figure 3c) in spite of focal parenchymal atrophy. This probably reflects "low-grade" slowly progressing tissue changes that the technique is not sensitive enough to detect. Moreover, the prominence of cortical vein involvement in our three GNA11-SWS patients contrasted with the usual prominence of radial transmedullary vein involvement in GNAQ-SWS. This suggests that the intracranial vascular anomaly could be different in the two conditions. If MRI is unavailable, a CT scan without contrast agent perfusion could provide relevant diagnostic information because of its high sensitivity in detecting calcium deposits within diseased areas, as illustrated by Patient #2 (Figure 3a).

Our three patients with SWS + CMO/U had a somatic hotspot *GNA11* mutation. One patient with the same *GNA11* mutation was reported with a post mortem neuropathological diagnosis of "meningeal angiomatosis/clinical suspicion" of SWS [11]. The lack of clinical images of the CM, of radiological imaging, and the notion of hyper- or hypertrophy in this report hinders the comparison with our patients and the establishment of a definite diagnosis. Another case described on the basis of the clinical picture as SWS with a somatic *GNA11* mutation had a pale reticulated and telangiectatic whole-body CM with hypotrophy of the right face and right leg, and concurrent glaucoma, analogous to our patients [12]. The leg CM was purple by 6 years of age. Brain MRI/magnetic resonance angiography did not detect any leptomeningeal angiomatosis, but SWI or contrast-enhanced FLAIR sequences were not mentioned. Thus, this patient does not fit the clinical criteria of SWS, yet the presentation seems to belong to the spectrum of *GNA11*-mutated CMs with over- or undergrowth [23]. In a series of 11 patients with "phacomatosis pigmentovascularis", a group of sporadic disorders in which pigmentary cutaneous lesions are associated with vascular malformations, four had a GNA11 mutation, one of whom had glaucoma, but no neurological anomaly [14]. No clinical picture or description of the CM or the age of the patient was published. Moreover, no brain MRI information or description of imaging modalities was given, rendering it impossible to compare the clinical phenotype with that of our patients.

GNAQ and *GNA11*-mutated SWS are clinically different. In the initial report on the genetic basis of SWS, 88% of the patients (n = 23/26) had a *GNAQ* mutation [10] and dark homogeneous CM, with usual occurrence of nodules and progressive soft tissue hypertrophy of the face leading to a significant dysmorphism. In our series, all three GNA11-SWS patients had a patchy and reticulated CM, which was pale at birth and slowly darkened over time, with rare appearance of nodules and limited hypertrophy. Moreover, the radiological features detected by brain MRI were more limited in our patients with GNA11-SWS than in patients with classic SWS, and they were diagnosed later in life. Therefore, two distinct entities exist—GNAQ-SWS and GNA11-SWS—with a different clinical presentation and course. GNA11-SWS can develop slowly in infancy or even only in adulthood. In a series of 628 patients with a diagnosis of SWS, delayed diagnosis was made after 1 year in 16% of cases [24]. These patients had mild neurological symptoms such as headaches,

vestibular or ear anomalies and were undiagnosed for years. Our three patients developed neurological symptoms after 1 year, had poor seizure control and the radiological diagnosis was more challenging than in GNAQ-SWS. Patients with delayed diagnosis and who have had symptoms for >1 year, may have GNA11-SWS.

The identification of the genetic bases of vascular malformations is becoming increasingly important and will help provide a precise diagnosis and prognosis. The identification of two SWS subgroups is a good example of this. As a single gene can cause variable phenotypes, it remains essential to associate the genetic underpinnings with the clinical features. Thus, we suggest the two SWS subtypes be termed GNA11-SWS and GNAQ-SWS, for better distinction. Such genetic-linked phenotypic diagnoses become fundamental as drug therapies are being developed for the management of patients with vascular anomalies, and differences in molecular pathophysiology can influence responses to therapies. These data suggest the importance of the use of FLAIR and SWI-BOLD when T1/T2-weighted MRI imaging is negative in patients with suspected SWS. If lesions are identified, anti-epileptic medication or future targeted therapies may be useful, as is the case in classic SWS.

AUTHOR CONTRIBUTIONS

Anne Dompmartin: Conceptualization (equal); data curation (equal); formal analysis (equal); investigation (equal); methodology (equal); writing – review and editing (equal). **Carine J. M. van der Vleuten:** Conceptualization (equal); data curation (equal); formal analysis (equal); investigation (equal); methodology (equal); writing – original draft (equal); writing – review and editing (equal). **Valerie Dekeuleneer:** Conceptualization (equal); data curation (equal); formal analysis (equal). **Thierry Duprez:** Conceptualization (equal); data curation (equal); formal analysis (equal); writing – original draft (equal). **Nicole Revencu:** Formal analysis (equal); investigation (equal); writing – original draft (equal); writing – review and editing (equal). **Julie Desir:** Data curation (equal); formal analysis (equal); writing – original draft (equal); writing – review and editing (equal). **D. Maroeska W. M. te Loo:** Data curation (equal); formal analysis (equal); writing – original draft (equal); writing – review and editing (equal). **Uta Flucke:** Data curation (equal); formal analysis (equal); writing – original draft (equal); writing – review and editing (equal). **Astrid Eijkelenboom:** Data curation (equal); formal analysis (equal); writing – original draft (equal); writing – review and editing (equal). **Leo Schultze Kool:** Formal analysis (equal); supervision (equal); validation (equal); writing – original draft (equal); writing – review and editing (equal). **Miikka Vikkula:** Conceptualization (equal); data curation (equal); formal analysis (equal); investigation (equal); methodology (equal); project administration (equal); resources (equal); software (equal); supervision (equal); validation (equal); visualization (equal); writing (draft preparation, review). **Laurence Boon:** Conceptualization (equal); data curation (equal); formal analysis (equal); investigation (equal); methodology (equal); project administration (equal); resources (equal); software (equal); supervision (equal); validation (equal); visualization (equal); writing – original draft (equal); writing – review and editing (equal).

ACKNOWLEDGMENTS

The authors thank Audrey Debue for expert technical assistance. These studies were financially supported by the *Fonds de la Recherche Scientifique* - FNRS grants T.0026.14 (to M.V.) and T.0146.16 (to L.B.) and the Fund Generet managed by the King Baudouin Foundation (to M.V.). The authors thank the Genomics Platform of University of Louvain for IonTorrent PGM Next Generation Sequencing. We also thank the National Lottery, Belgium, and the Foundation against Cancer (2010-101), Belgium for their support for the Genomics Platform of University of Louvain and de Duve Institute, as well as the *Fonds de la Recherche Scientifique* - FNRS equipment grant U.N035.17 for the "Big data analysis cluster for NGS at UCLouvain". Nine of the authors of this publication are members of the Vascular Anomalies Working Group (VASCA WG) of the European Reference Network for Rare Multisystemic Vascular Diseases (VASCERN): Project ID: 769036.

CONFLICT OF INTEREST

The authors declare no conflict of interest.

DATA AVAILABILITY STATEMENT

Data are not provided in the article because of space limitations. They may be shared (anonymized) at the request of any qualified investigator for purposes of replicating procedures and results.

ORCID

Anne Dompmartin https://orcid.org/0000-0003-0081-500X
Carine J. M. van der Vleuten https://orcid.org/0000-0002-0641-7072
Valérie Dekeuleneer https://orcid.org/0000-0003-1210-6112
Thierry Duprez https://orcid.org/0000-0002-1579-0100
Nicole Revencu https://orcid.org/0000-0002-7120-4903
Julie Désir https://orcid.org/0000-0002-1998-0761
D. Maroeska W. M. te Loo https://orcid.org/0000-0001-6308-4801
Uta Flucke https://orcid.org/0000-0003-0315-4307
Astrid Eijkelenboom https://orcid.org/0000-0001-8264-8131
Leo Schultze Kool https://orcid.org/0000-0001-9217-278X
Miikka Vikkula https://orcid.org/0000-0002-6236-338X
Laurence Boon https://orcid.org/0000-0001-8273-3328

REFERENCES

1. Wassef M, Blei F, Adams D, et al. Vascular anomalies classification: recommendations from the International Society for the Study of vascular anomalies. *Pediatrics*. 2015;136(1):e203-e214. doi:10.1542/peds.2014-3673
2. Waelchli R, Aylett SE, Robinson K, Chong WK, Martinez AE, Kinsler VA. New vascular classification of port-wine stains: improving prediction of Sturge-weber risk. *Br J Dermatol*. 2014;171(4):861-867. doi:10.1111/bjd.13203
3. Rujimethapass N, Manuskiatti W, Wanitphakdeedecha R, Petchyim S. Ocular manifestations of facial port-wine stain, nevus of Ota, and phakomatosis pigmentovascularis in Asian patients. *J Am Acad Dermatol*. 2021;85(5):1194-1200. doi:10.1016/j.jaad.2020.04.169
4. Lo W, Marchuk DA, Ball KL, et al. Brain vascular malformation consortium National Sturge-Weber Syndrome Workgroup. Updates

and future horizons on the understanding, diagnosis, and treatment of Sturge-weber syndrome brain involvement. *Dev Med Child Neurol*. 2012;54(3):214-223. doi:10.1111/j.1469-8749.2011.04169.x
5. Bachur CD, Comi AM. Sturge-weber syndrome. *Curr Treat Options Neurol*. 2013;15(5):607-617. doi:10.1007/s11940-013-0253-6
6. Greene AK, Taber SF, Ball KL, Padwa BL, Mulliken JB. Sturge-weber syndrome: soft-tissue and skeletal overgrowth. *J Craniofac Surg*. 2009;20(Suppl 1):617-621. doi:10.1097/SCS.0b013e318192988e
7. Limaye N, Wouters V, Uebelhoer M, et al. Somatic mutations in angiopoietin receptor gene TEK cause solitary and multiple sporadic venous malformations. *Nat Genet*. 2009;41(1):118-124. doi:10.1038/ng.272
8. Dekeuleneer V, Seront E, Van Damme A, Boon LM, Vikkula M. Theranostic advances in vascular malformations. *J Invest Dermatol*. 2020;140(4):756-763. doi:10.1016/j.jid.2019.10.001
9. Queisser A, Seront E, Boon LM, Vikkula M. Genetic basis and therapies for vascular anomalies. *Circ Res*. 2021;129(1):155-173. doi:10.1161/CIRCRESAHA.121.318145
10. Shirley MD, Tang H, Gallione CJ, et al. Sturge-weber syndrome and port-wine stains caused by somatic mutation in GNAQ. *N Engl J Med*. 2013;368(21):1971-1979. doi:10.1056/NEJMoa1213507
11. Thorpe J, Frelin LP, McCann M, et al. Identification of a mosaic activating mutation in GNA11 in atypical Sturge-weber syndrome. *J Invest Dermatol*. 2021;141(3):685-688. doi:10.1016/j.jid.2020.03.978
12. Polubothu S, Al-Olabi L, Carmen Del Boente M, et al. GNA11 mutation as a cause of Sturge-weber syndrome: expansion of the phenotypic spectrum of $G_{\alpha/11}$ mosaicism and the associated clinical diagnoses. *J Invest Dermatol*. 2020;140(5):1110-1113. doi:10.1016/j.jid.2019.10.019
13. Jordan M, Carmignac V, Sorlin A, et al. Reverse phenotyping in patients with skin capillary malformations and mosaic GNAQ or GNA11 mutations defines a clinical spectrum with genotype-phenotype correlation. *J Invest Dermatol*. 2020;140(5):1106-110.e2. doi:10.1016/j.jid.2019.08.455
14. Thomas AC, Zeng Z, Rivière J-B, et al. Mosaic activating mutations in GNA11 and GNAQ are associated with phakomatosis pigmentovascularis and extensive dermal melanocytosis. *J Invest Dermatol*. 2016;136(4):770-778. doi:10.1016/j.jid.2015.11.027
15. Limaye N, Kangas J, Mendola A, et al. Somatic activating PIK3CA mutations cause venous malformation. *Am J Hum Genet*. 2015;97(6):914-921. doi:10.1016/j.ajhg.2015.11.011
16. Sudarsanam A, Ardern-Holmes SL. Sturge-weber syndrome: from the past to the present. *Eur J Paediatr Neurol*. 2014;18(3):257-266. doi:10.1016/j.ejpn.2013.10.003
17. Sabeti S, Ball KS, Burkhaart C, et al. Consensus statement for the management and treatment of por-wine birthmarks in Sturge-Weber syndrome. *JAMA Dermatol*. 2021;157(1):98-104.
18. Comi AM, Bellamkonda S, Ferenc LM, Cohen BA, Germain-Lee EL. Central hypothyroidism and Sturge-weber syndrome. *Pediatr Neurol*. 2008;39(1):58-62. doi:10.1016/j.pediatrneurol.2008.03.018
19. Lee MS, Liang MG, Mulliken JB. Diffuse capillary malformation with overgrowth: a clinical subtype of vascular anomalies with hypertrophy. *J Am Acad Dermatol*. 2013;69(4):589-594. doi:10.1016/j.jaad.2013.05.030
20. Goss JA, Konczyk DJ, Smits P, et al. Diffuse capillary malformation with overgrowth contains somatic PIK3CA variants. *Clin Genet*. 2020;97(5):736-740. doi:10.1111/cge.13702
21. Juhasz C, Haacke EM, Hu J, et al. Multimodality imaging of cortical and white matter abnormalities in Sturge-Weber syndrome. *Am J Neuroradiol (AJNR)*. 2007;28:900-906.
22. Hu J, Yu Y, Juhasz C, et al. MR susceptibility weighted imaging [SWI] complements conventional contrast-enhanced T-1 weighted MRI in characterizing brain abnormalities of Sturge-weber syndrome. *J Magn Reson Imaging*. 2008;28:300-307.
23. Couto JA, Ayturk UM, Konczyk DJ, et al. A somatic GNA11 mutation is associated with extremity capillary malformation and overgrowth. *Angiogenesis*. 2017;20(3):303-306. doi:10.1007/s10456-016-9538-1
24. Cho S, Maharathi B, Ball KL, Loeb JA, Pevsner J. Sturge-Weber syndrome patient registry: delayed diagnosis and poor seizure control. *J Pediatr*. 2019;215:158-63.e6. doi:10.1016/j.jpeds.2019.08.025

How to cite this article: Dompmartin A, van der Vleuten CJM, Dekeuleneer V, et al. GNA11-mutated Sturge–Weber syndrome has distinct neurological and dermatological features. *Eur J Neurol*. 2022;00:1-10. doi: 10.1111/ene.15452